Received: 4 June 2021 | Revised: 9 October 2021 | Accepted: 9 October 2021 | Published on: 2 November 2021

DOI: 10.1002/joc.7414

RESEARCH ARTICLE

International Journal of Climatology RMetS

North Atlantic air pressure and temperature conditions associated with heavy rainfall in Great Britain

Andrew Paul Barnes[1] | **Cecilia Svensson**[2] | **Thomas Rodding Kjeldsen**[1]

[1]Department of Architecture and Civil Engineering, University of Bath, Bath, UK

[2]UK Centre for Ecology & Hydrology, Wallingford, UK

Correspondence
Andrew Paul Barnes, Department of Architecture and Civil Engineering, University of Bath, Bath, UK.
Email: apb41@bath.ac.uk

Funding information
Engineering and Physical Sciences Research Council, Grant/Award Number: EP/L016214/1; Natural Environment Research Council, Grant/Award Number: NE/R016429/1; UK-SCAPE

Abstract

Severe flooding in the United Kingdom is often linked to the occurrence of heavy rainfall events, which can be characterized by the synoptic scale meteorological conditions over the North Atlantic region. Seasonal heavy rainfall events (summer and winter 1-day maxima) were extracted from 125 locations across Great Britain over the period 1950–2017. For each event, anomaly sea-level pressure and 2 m air temperature conditions across the North Atlantic sector were extracted. In contrast to earlier studies, these two datasets were combined and clustered to identify how the pressure and temperature conditions co-vary within each half-year to produce heavy rainfall events. Distinctly different spatial patterns were found for four classes in summer and for three classes in winter. For all classes there is a negative sea-level pressure anomaly centred over or near the British Isles. However, whereas in summer the low pressures are associated with either predominantly cold or warm anomalies over most of the North Atlantic, in winter two phases of a smaller-scale four-pole temperature pattern emerges. Nevertheless, for one of the winter classes the cold anomaly over the northwest Atlantic is so deep, persistent and widespread that, unusually for the winter season, a significant relationship between the class's frequency of occurrence and the Atlantic Multidecadal Oscillation (AMO) index is found ($r = -.39$). Further, for both seasons heavy rainfall occurs when the AMO and the North Atlantic Oscillation (NAO) are in opposing phases. Particularly, positive NAO and negative AMO result in heavy rainfall in western Britain. Two classes in each season are consistent with positive and negative phases of the NAO, and the two non-NAO summer classes are associated with a northward extension of the subtropical high pressure and heavy rainfall in the southeast. The association between heavy rainfall and large-scale circulation and temperature drivers can find application in, for example, weather generators.

KEYWORDS

AMO, classification, heavy rainfall, NAO, sea level pressure, temperature

1 | INTRODUCTION

The impacts of extreme weather across the UK continue to have severe economic and environmental consequences. The cost of flood damage, often a result of heavy rainfall, is expected to increase significantly in the future, unless an average annual investment of £1 bn is made (with a benefit to cost ratio of 9:1) to protect properties and infrastructure in England up to 2065 (LTIS, 2019). The danger to life can be shown by, for example, storms Dennis and Ciara which hit the UK during February of 2020 and resulted in at least 5 fatalities and more than £300mil in damages (Griffith, 2020). Considering the risk to life and property, there is an inherent reason to try to better understand the synoptic-scale mechanisms behind heavy rainfall. However, with the climate also expected to change in future, and current climate models being better at predicting large-scale circulation patterns rather than heavy rainfall magnitudes, these patterns of large-scale forcings have received renewed attention as a research topic. Specifically, the aim of this study is to identify the key types of synoptic-scale meteorological patterns, which cause heavy rainfall events in the UK.

Taylor and Yates (1967) reviewed several weather and climate classification schemes based on the atmospheric pressure pattern in the region around the UK. They found that the existing procedures were rather arbitrary and the methods almost indistinguishable from each other. Currently, the most popular weather typology, by Lamb (1972), consists of manually classified weather records from 1861 to 1971 based on their airflow patterns. Although Lamb's types contain 27 categories in total, the bulk of the records belong to one of seven main types of air flow classification: cyclonic, anticyclonic, northerly, easterly, westerly, north westerly and southerly (Lamb, 1965, 1972). Originally, these weather types were determined subjectively until Jenkinson and Collison (1977) turned this into an objective classification scheme by using mean daily grid-point sea-level pressure. More recently, researchers have extended the area of influence and/or used objective methods for classification to try to capture the synoptic scale processes which create weather events in the UK. For example, Fereday *et al*. (2008) use *k*-means clustering of sea level pressures (SLP) over the North Atlantic to identify the SLP profiles for a set of 6 two-month seasons. However, they were unable to identify any common circulation types. Neal *et al*. (2016) identified eight distinct weather patterns which were reduced from an original set of 30 classes through clustering on the anomaly sea-level pressure patterns. Richardson *et al*. (2017) compared the precipitation of events classified in each of the classes generated by Neal *et al*. (2016) and found the reduced set of eight classes to show very high intra-class precipitation variability. It may be that including information also of moisture availability could make for a more distinct classification scheme.

In a recent review, Gimeno *et al*. (2020) highlights that the key sources of European moisture come from the North Atlantic through either atmospheric rivers or cyclonic activity. Lavers *et al*. (2011) first identified atmospheric rivers by investigating the source regions of the atmospheric moisture feeding heavy rainfalls in the UK. Lavers *et al*. (2011) found that all ten of the largest floods in the UK co-occurred with an atmospheric river. These atmospheric rivers are long plumes of high-concentrations of water vapour in the atmosphere which originate from the tropics, moving northwards into the mid-latitudes. However, the concept and definition of an atmospheric river still does not provide clear evidence of the synoptic scale driving process. Further to this, the atmospheric river contribution to rainfall mainly occurs during the winter half year when extratropical cyclones (within which atmospheric rivers occur) are more prevalent (Lavers and Villarini, 2015) and hence do not explain summer extremes.

Allan *et al*. (2019) investigated synoptic precursors of extreme short-duration (3-hr) summer rainfall events in the UK, including dew point temperature, evaporation, geopotential height at 200 hPa and sea-level pressure (SLP) anomalies, geopotential height anomalies, average moisture and evaporation patterns over northwest Europe and the North Atlantic. Their results reveal different conditions associated with intense rainfall events in different parts of the country. For example, intense rainfall events in both the South East of England and western Scotland coincide with negative SLP anomalies in the eastern Atlantic on the day prior to the event. However, for intense rainfall events in the South East of England the centre of this negative SLP anomaly is further south than for events in western Scotland. Their results highlight not only the regional homogeneity of extreme events (e.g., Champion *et al*., 2019; Svensson and Hannaford, 2019) in the UK but also their association with particular synoptic scale atmospheric patterns. Similarly, Ummenhofer *et al*. (2017) clustered SLP and precipitation patterns over Europe and identified a similar northwest and southeast regional disparity across the British Isles.

Alternative methods for investigating moisture sources have included using small-scale air parcel tracking to generalize the key moisture pathways leading to extreme events (Santos *et al*., 2018; Tan *et al*., 2018; Barnes *et al*., 2019a; Barnes *et al*., 2019b). These methods provide only the general movement of moisture in the atmosphere, but Barnes *et al*. (2019b) identified six

distinct groups of moisture pathways leading to events in the UK. The key differences between the pathways were length and direction of travel, but the results also showed that the distributions of rainfall intensity varied between groups, and spatially across the country.

Several studies have found that temperature and circulation pattern influence rainfall magnitude. For example, for southern Italy Greco *et al.* (2020) highlight the importance of low-level (850 hPa) temperature for the development of precipitation from convective systems while synoptic system precipitation depend on the pressure pattern. For the UK Blenkinsop *et al.* (2015) also found a positive relationship between precipitation and (local land surface) temperature during summer, but note that such relationships were weaker in the remaining seasons. Tramblay *et al.* (2013) built a rainfall frequency model for southern France using temperature and pressure patterns as co-variates for the model parameters.

The present study investigates the combined effects of synoptic 2 m air temperature and sea level pressure patterns in the North Atlantic region on heavy rainfall occurrence across Great Britain. Temperature is used instead of moisture, as initial investigations suggested a strong relationship between the two over the ocean. By using such a proxy, both moisture over the ocean as well as temperature over the land can be captured by a single variable, which simplifies our large-scale analysis. We use a technique to simultaneously cluster both 2 m air temperature and sea level pressure patterns across the North Atlantic sector during heavy rainfall events. As far as the authors are aware, this combined clustering expands on all earlier weather typing studies for the area. The clustering results in a range of combined synoptic patterns, instead of a single composite pattern for each driver separately as in, for example, the detailed sub-daily summer rainfall studies of Allan *et al.* (2019) and Champion *et al.* (2019). Further, we investigate winter as well as summer, but look at the coarser resolution of 1-day rather than 3-hr rainfall events. An advantage of using daily rather than sub-daily rainfall data is the higher confidence in the data quality. In contrast to, for example, Ummenhofer *et al.* (2017), the synoptic patterns are used to identify differences in geographical extreme rainfall distribution, as opposed to including the spatial rainfall pattern as part of the clustering. The average wind speeds/directions and 500 hPa geopotential height pattern for each class are also investigated. Finally, the present study relates the synoptic patterns to time and climatic indices such as the North Atlantic Oscillation (NAO) and the Atlantic Multidecadal Oscillation (AMO), to investigate how long-term oscillations may influence what synoptic temperature and pressure patterns cause heavy rainfalls in different parts of Great Britain.

2 | DATA

Two types of data were used in this study: (1) individual time series of seasonal (half-year) maximum 1-day rainfalls at 125 locations in Great Britain, and (2) large-scale gridded daily values of sea level pressure and air temperature data over the North Atlantic sector.

2.1 | Historical heavy rainfall events

Time series of heavy rainfall were extracted at 125 locations as shown in Figure 1, chosen at equal 0.5° latitude and longitude spacing. This equates to ~35 km, depending on latitude. Although gridded rainfalls are likely to lose some variability compared with using station observations, they enable us to extract rainfalls on an even grid across Great Britain. Seasonal maximum daily rainfall (SMAX) series for both summer (May–Oct) and winter (Nov–Apr) seasons were retrieved for each location from the CEH-GEAR (Centre of Ecology and Hydrology – Gridded Estimates of Areal Rainfall) (Tanguy *et al.*, 2019) dataset for the years 1950 up to and including 2017. The CEH-GEAR data uses a nearest neighbour interpolation method on observed precipitation data from the Met Office, to create a 1 km × 1 km cell grid of daily (09:00 UTC to 09:00 UTC) total precipitation across the United Kingdom. This grid is then normalized using average annual rainfall and subsequently adjusted by monthly rainfall averages as described by Keller *et al.* (2015).

Combining the seasonal maximum series results in a total of (68 years * 125 locations=) 8,500 seasonal heavy rainfall events. The first winter of the study period is only 4-months long (Jan-Apr), and Nov-Dec 2017 is not included in the analysis. Of the 8,500 summer heavy events there are 2,282 unique dates on which they occur. Similarly, for the 8,500 winter heavy events there are 2010 unique dates. This is expected as locations within the same hydrometeorological region are influenced by the same atmospheric circumstances (Keef *et al.*, 2009; Champion *et al.*, 2019) and therefore spatial dependence will lead to a level of co-occurrence on the same day. Unless stated, the rest of the analysis is carried out using the series of unique dates, to ensure that a single widespread event does not disproportionately influence the results.

2.2 | Meteorological data

Daily (00:00 UTC to 00:00 UTC) mean sea level pressure (SLP) and 2 m air temperature (AT) data were extracted from the 2.5° gridded NCEP/NCAR Reanalysis 1 dataset (https://psl.noaa.gov/data/gridded/data.ncep.reanalysis.

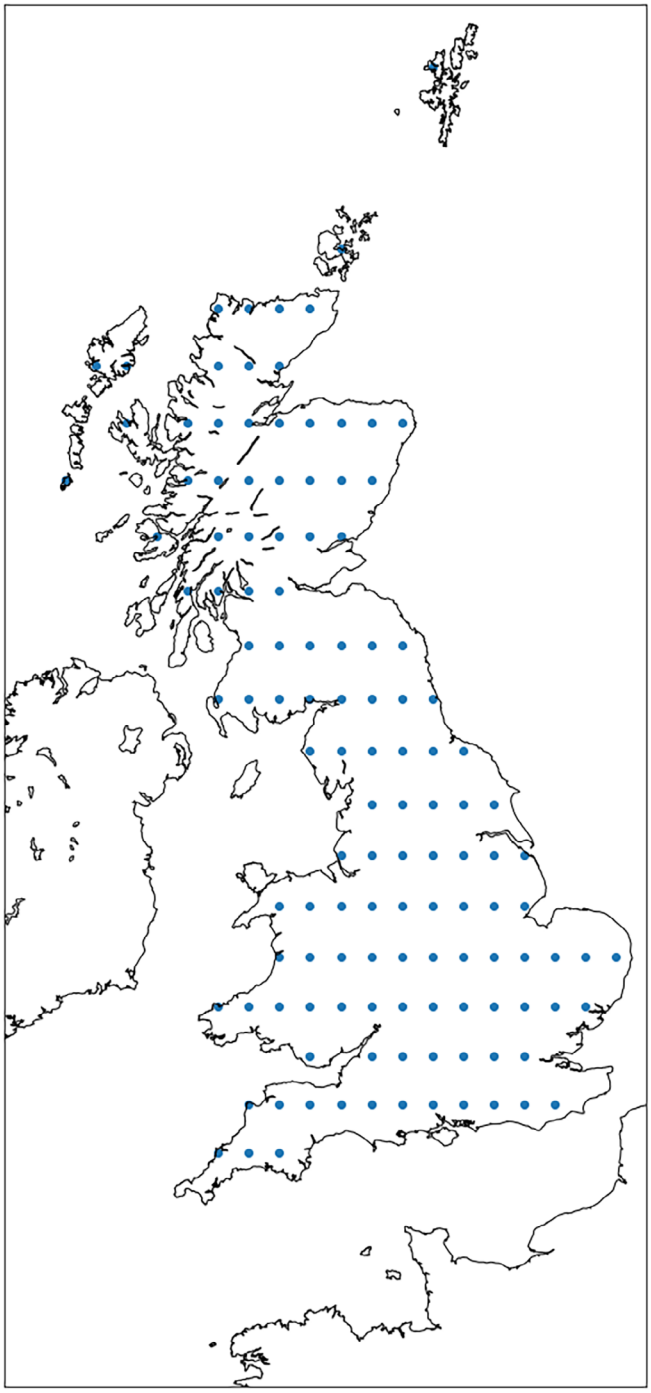

FIGURE 1 The 125 locations in Great Britain at which series of seasonal rainfall maxima are extracted [Colour figure can be viewed at wileyonlinelibrary.com]

html) (Kalnay *et al*., 1996). This means the daily meteorological data precede the rainfall days by several hours, but we consider the data sufficiently overlapping for our purpose. The study area is limited to the region defined by 10–70°N and −100 to 20°E, which covers the North Atlantic sector and part of the neighbouring land areas (see e.g., Figures 2 and 3). We chose to include Greenland and part of North America to see if the temperature patterns within the polar regions influenced the resulting winter classes. Similarly, we included part of North Africa to see if the temperature there would result in a separate summer cluster for a Spanish Plume mechanism. This means our study region is slightly larger than the one considered by, for example, Allan *et al*. (2019).

For each heavy rainfall date a SLP and AT pattern were generated, each with a resolution of 48 × 24 grid cells. Following this, each cell's daily value was then standardized by subtracting the monthly mean and subsequently dividing by the standard deviation of that cell's SLP or AT, respectively, with the mean and standard deviation calculated over all the daily values in all years for the calendar month in which the event occurred. Identical fields were extracted from the NCEP/NCAR Reanalysis 1 dataset also for wind components and 500 hPa geopotential heights, which were used to help with the interpretation of the resulting SLP and AT patterns.

To enable comparisons with larger scale climatic oscillations, the North-Atlantic Oscillation (NAO) (NOAA National Weather Service, 2005) and Atlantic Multidecadal Oscillation (AMO) (Enfield *et al*., 2001) indices are extracted seasonally for both summer and winter, 1950–2017. The NAO provided by NOAA (https://www.cpc.ncep.noaa.gov/products/precip/CWlink/pna/nao.shtml) is generated using a rotated principal components analysis as described by Barnston and Livezey (1987), which allows the location of the pressure centres to differ slightly from one season to another. The AMO, which is also provided by NOAA (https://psl.noaa.gov/data/timeseries/AMO/), is calculated using the weighted average over the North Atlantic sea-surface temperature of the Kaplan SST V2 dataset (https://psl.noaa.gov/data/gridded/data.kaplan_sst.html) (Kaplan *et al*., 1998).

3 | METEOROLOGICAL CLUSTERING

Clustering on a combination of the anomaly SLP and AT patterns is conducted to identify a set of distinct meteorological conditions associated with seasonal heavy rainfall events.

3.1 | Feature set preprocessing

For each unique heavy rainfall day extracted from the CEH-GEAR dataset, a single data array is generated by flattening and concatenating the anomaly SLP and AT matrix for that date. Each pixel in the meteorological dataset have a size of 2.5° × 2.5°, equating to an image of size 24 by 48 = 1,152 individual pixels. Because there are

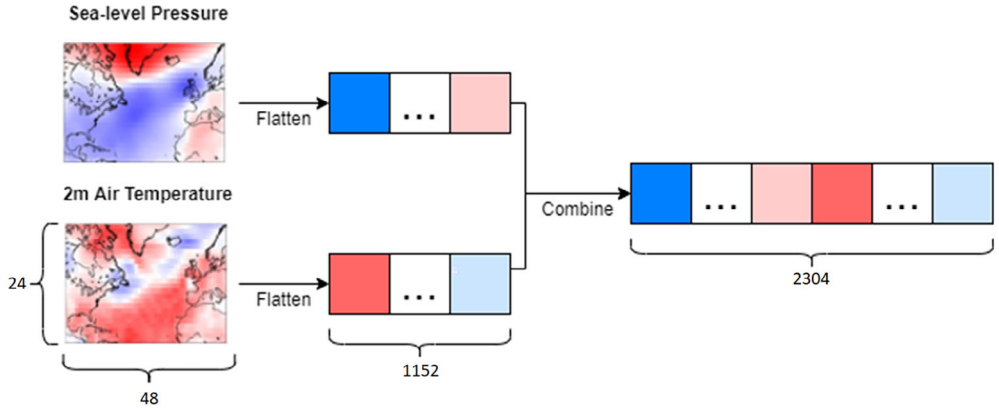

FIGURE 2 Example of feature set generation for a given heavy rainfall event. This procedure takes the SLP and AT patterns, flattens them into a single dimensional array and finally concatenates them into a final single dimensional array [Colour figure can be viewed at wileyonlinelibrary.com]

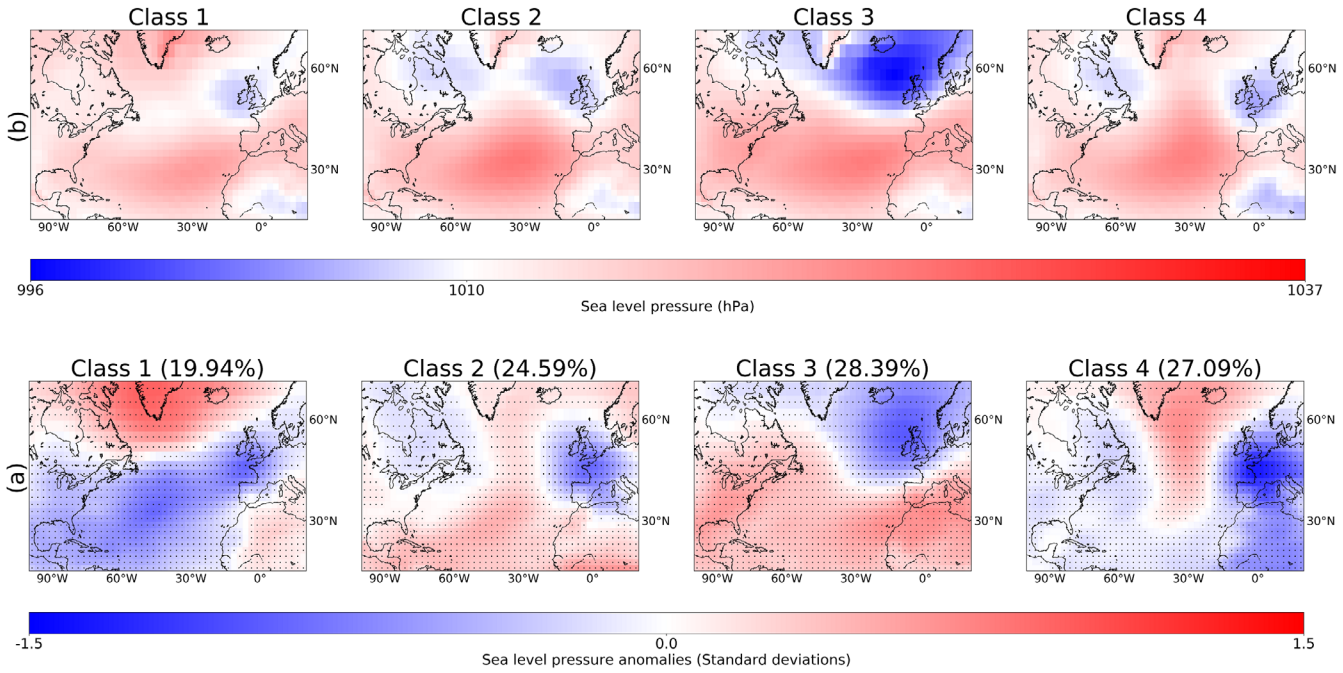

FIGURE 3 Sea level pressure patterns for the four summer classes, showing both the anomaly SLP (a) and raw SLP (b) patterns. The percentages indicate the proportion of events in each class, and the dots provided in (a) denote anomalies significant at the 2% level based on a two-sided Student's *t* test [Colour figure can be viewed at wileyonlinelibrary.com]

two meteorological images, this results in each heavy rainfall day being represented by a single vector of size (2*1152=) 2,304, referred to as the event's feature vector. An illustration of this procedure is shown in Figure 2, and an example is given for flattening in Equation (1) and combination in Equation (2).

$$Flatten\left(\begin{bmatrix} x_{1,1} & \cdots & x_{48,1} \\ \vdots & x_{i,j} & \vdots \\ x_{1,24} & \cdots & x_{48,24} \end{bmatrix}\right) = \left[x_{1,1},\cdots,x_{48,1},\cdots,x_{i,j},\cdots,x_{1,24}\cdots,x_{48,24}\right] = \left[x_1\cdots,x_{1152}\right] \tag{1}$$

$$Combine\left(\left[x_1,\cdots,x_m,\cdots,x_{1152}\right],\left[y_1,\cdots,y_n,\cdots,y_{1152}\right]\right) = \left[x_1,\cdots,x_m,\cdots,x_{1152},y_1,\cdots,y_n,\cdots,y_{1152}\right] \tag{2}$$

Combining the event feature vectors, separately for each season, results in 2 two-dimensional matrices where each row represents the date of a heavy rainfall event in the given season. These matrices are referred to as the training sets. The dimensions of the training set matrices are $[N \times 2{,}304]$ where 2,304 is the number of elements present in each heavy rainfall event feature set and N is the number of unique heavy rainfall days in the given season.

3.2 | Pattern clustering

The procedure used to class the feature sets defined in Section 3.1 is *k*-means (Lloyd, 1982) which requires a set number of output classes (*k*) to be pre-specified. Class models were generated for both summer and winter with *k* ranging from 2 to 15 which are limits based on the number of classes used by Neal *et al*. (2016) to allow for differences in the data. However, Richardson *et al*. (2017) show that only about four of Neal *et al*. (2016)'s 30 patterns relate to heavy rainfall events, which indicates that this may be a suitable number to consider. We found that plots of root-mean squared error (RMSE) versus number of clusters were not helpful for cluster selection in our case (not shown). As expected the RMSE drops with increasing number of clusters, but there is no clear break point, possibly because using the distance metrics on such high-dimensional data produce results which are often noisy (Aggarwal *et al*., 2001). Instead, we subjectively selected 3 classes for winter and 4 classes for summer.

3.3 | Statistical analysis

We used correlation analysis to explore if the frequency of occurrence of events in the identified classes is related to the NAO and AMO climate indices. For this, we used seasonally averaged indices of the NAO and AMO, and seasonal counts of the number of events in each class. Before the correlation analysis was undertaken, each series was detrended. That is, the correlation analysis was undertaken on the residuals from linear regressions of each variable separately on time. *p*-values were estimated using a two-sided Student's *t* test, and unless otherwise stated a significance level of 5% was used.

4 | RESULTS

This section presents the results of the class analysis of the daily anomaly sea-level pressure and 2 m air temperatures across the North Atlantic sector, for the dates which coincide with heavy rainfall events in Great Britain. Presented below are the mean anomaly sea-level pressures and 2 m air temperatures for each cluster, shown separately for summer and winter. The average wind speeds/directions and 500 hPa geopotential height pattern for each class are also discussed. The relationship between the frequency of occurrence of the events in each class and indices of the NAO, AMO and time are then investigated. Finally, the classes are compared for their spatial distribution of the heavy rainfall events across Great Britain.

4.1 | Summer classes

4.1.1 | Meteorological conditions

Figure 3 shows both the anomaly and raw SLP patterns for the four summer classes generated using *k*-means. Each class is represented by the mean of all patterns which are classified under the respective cluster. Common across all four classes is an area of low pressure anomaly centred on, or to the north of, the British Isles. In addition, Classes 1, 2 and 4 share a dominant high SLP anomaly through Greenland and the Norwegian sea, with Classes 1 and 4 also showing a low SLP anomaly from the subtropical North Atlantic to northwest Europe. In contrast, Classes 2 and 3 present a dominant high SLP anomaly pattern across the sub-tropical Atlantic. Classes 1 and 3 largely reflect the expected anomaly patterns of the negative and positive phases of the summer NAO, respectively, with one anomaly centre over Iceland and another to the southeast over the North Atlantic/Europe (Figure 3a). Compared with the north–south gradient of the winter NAO (e.g., Jones *et al*., 1997), the gradients of Classes 1 and 3 are slightly rotated counter-clockwise, which is typical of the summer NAO as described by, for example, Folland *et al*. (2009). The two classes for which an NAO interpretation is less obvious (Classes 2 and 4), seem to be associated with a northward extension of the positive anomalies of the subtropical high pressure. This is shown as a north–south band of high SLP anomalies in the mid-Atlantic in Figure 3a.

Considering the 2 m air temperature anomalies as shown in Figure 4, the classes can be split into anomalously warm and cool patterns with Classes 1 and 2 presenting a generally warm North Atlantic region and Classes 3 and 4 showing a predominantly cool pattern. Common to all four classes is that there is an area of cold anomalies to the west or northwest of the UK, which contrasts with a warmer anomaly to the southeast. This could signify the temperature contrast over a cold front, which would typically result in heavy rainfall as it passes eastwards across the UK.

The average wind vectors (superimposed in Figure 4) of the relevant classes show the presence of cyclonic activity near the British Isles, along with the indication of anti-cyclonic activity in the subtropical North Atlantic. The winds associated with the northward extended subtropical high pressure for Classes 2 and 4 presumably contributes to the development of the warm (cold) anomaly in the west (east) mid-latitude Atlantic. The direction of flow for the low temperature zones to the west and/or northwest of the British Isles has a northerly component for all four classes and is sometimes directed towards the British Isles.

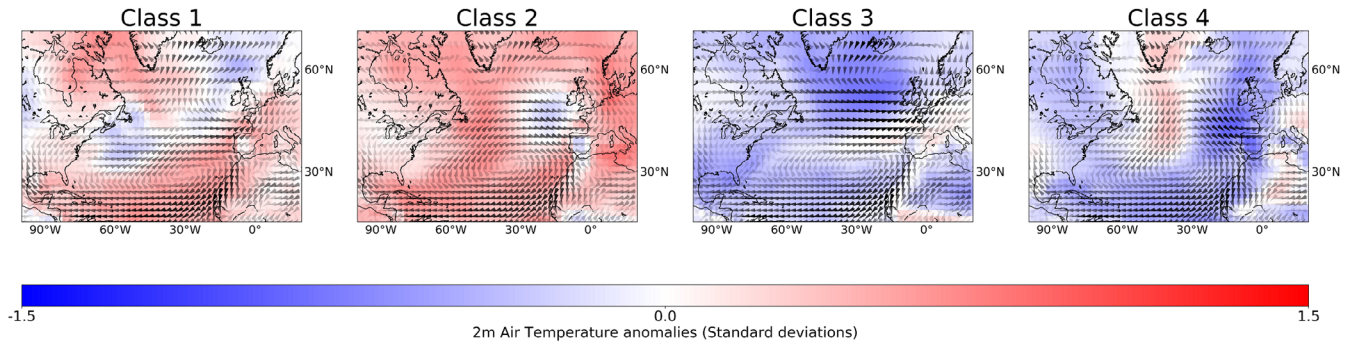

FIGURE 4 Sea-level wind speeds for summer classes. The sea-level wind speeds are overlaid on the anomaly temperature patterns for each of the four summer classes, and the opacity illustrates the strength of wind between 2 and 8 m/s. Anomaly 2 m air temperature patterns are shown without wind speeds, but with points denoting significance, in Supplementary Information S1 [Colour figure can be viewed at wileyonlinelibrary.com]

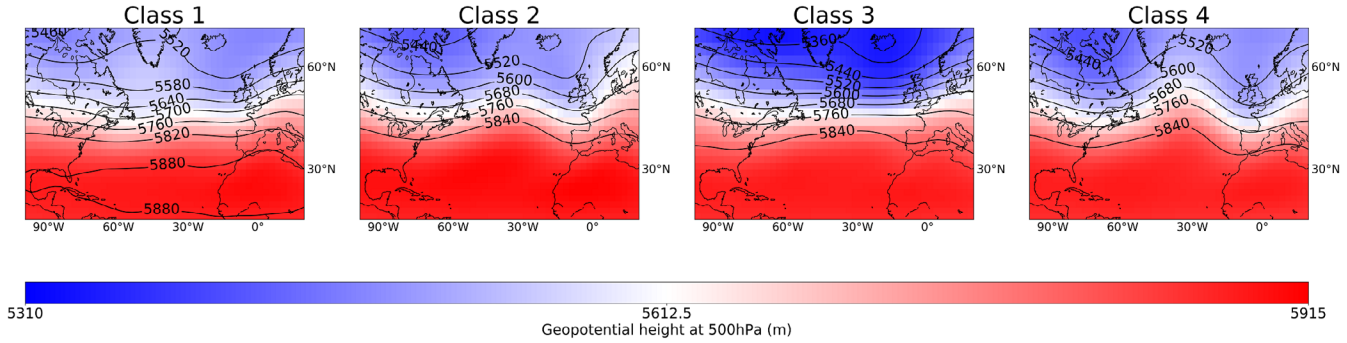

FIGURE 5 500 hPa geopotential heights for each summer class [Colour figure can be viewed at wileyonlinelibrary.com]

The 500 hPa geopotential height fields shown in Figure 5 indicate the directions of the paths travelled by the mid-latitude cyclones that cause the heavy rainfall events, even though they do not show the exact location of the jet stream. Cyclones are steered by the airflow aloft, which is parallel to the isolines of the geopotential heights. The strong north–south contrast and zonal pattern for Class 3 suggest storms are fast-moving on a straight, westerly track across the Atlantic, turning northeastward in the vicinity of the UK. Classes 2 and 4 suggest strongly meandering storm tracks (as also suggested by the northward extension of the subtropical high pressure in Figure 3), whereas Class 1 storm tracks seem more weakly meandering.

4.1.2 | Class variability

The top row of Figure 6 shows how the frequency of occurrence of the events in each summer class varies with time, while the lower two rows show how the detrended frequencies of occurrence vary with the detrended indices of the NAO and AMO. The frequencies of Classes 1 and 2 both increase with time, whereas the frequency of Class 4 decreases and Class 3 shows no significant temporal trend.

The events in Class 3, whose pressure pattern resembles the positive phase of the summer NAO, show directly opposite relationships with the NAO and the AMO to those of Class 1, all significant at the 5% level. This suggests that heavy rainfalls associated with the positive (negative) phase of the NAO is exacerbated by cold (warm) temperatures in the North Atlantic. A possible explanation for this would be the different tracks that storms associated with the positive and negative phases of the NAO track along, and the development of different rainfall-exacerbating sea surface temperature anomalies in the vicinity of Britain. The sea surface temperature anomaly will in turn modify the temperature of the overlying airmass. For example, the locations of the low pressure centres in Figure 3 suggest a more northward location of storms for the positive NAO Class 3 than for the negative NAO Class 1. Class 3 cyclones tracking eastward to the north of Scotland will drive cold waters behind themselves towards Britain and warmer waters ahead of themselves northward, where they will not

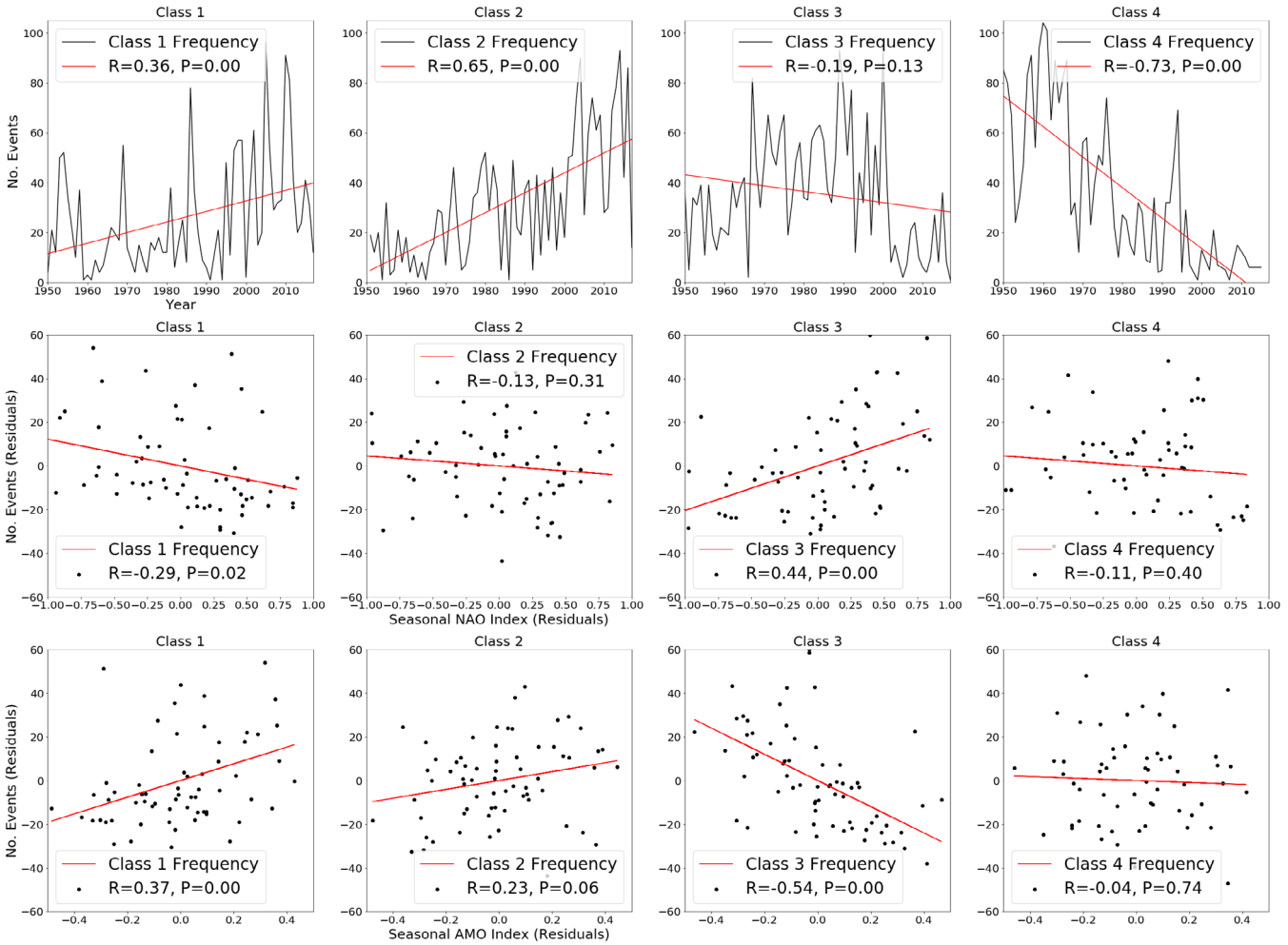

FIGURE 6 Seasonal frequency of occurrence of heavy rainfall events in the four summer classes as function of time (top row), and detrended seasonal frequencies as a function of detrended NAO index (middle row) and AMO index (bottom row). The figure also shows the correlation coefficient, *R*, and its associated *p*-value (*P*) [Colour figure can be viewed at wileyonlinelibrary.com]

affect Britain. Further, the aggregated action of a succession of cyclones following a similar path may exacerbate a developing sea surface temperature anomaly. Hence, when the Atlantic is anomalously cold and the NAO is positive, the cold anomaly to the northwest of Britain will be exacerbated (Figure 4, Class 3), and this will also be reflected in the air temperature anomaly.

In contrast, storms tracking along a path further to the south will drive warm surface waters ahead of themselves towards Britain, while a cold sea surface anomaly will be generated behind the low-pressure centres (Figure 4, Class 1). Therefore, when the Atlantic is anomalously warm and the NAO is in its negative phase, the warm anomaly to the south of Britain will be exacerbated. There is some support for this in Figure 7, when contrasting the temporal evolution of the temperature anomaly patterns for Class 1 (negative NAO) with those for Class 3 (positive NAO). For Class 1, and to some extent also for Class 2, the warm anomaly off North Africa and western Europe intensifies and moves northward towards Britain in the days prior to the heavy rainfall event occurring, while a weak cold anomaly forms to the northwest, behind the cyclone. However, for Class 3 the cold anomaly that develops to the northwest of Britain is more intense than the anomaly over and around Britain. In this case, the cold anomalies west of North Africa and western Europe seem to be unchanging in the days prior to the heavy rainfall. Supplementary Information S3 shows the corresponding development of sea level pressure anomalies in the days prior to the heavy rainfall event.

Both Classes 2 and 4 seem to be associated with a northward extension of the subtropical high pressure in the North Atlantic (Figure 3), and the 500 hPa geopotential height patterns in Figure 5 support the suggestion of highly meandering storm tracks. Cyclones following such paths are likely to be slow-moving, which enables the accumulation of very large rainfall amounts. Figure 8 suggests that storms in these two classes result in heavy rainfall mainly

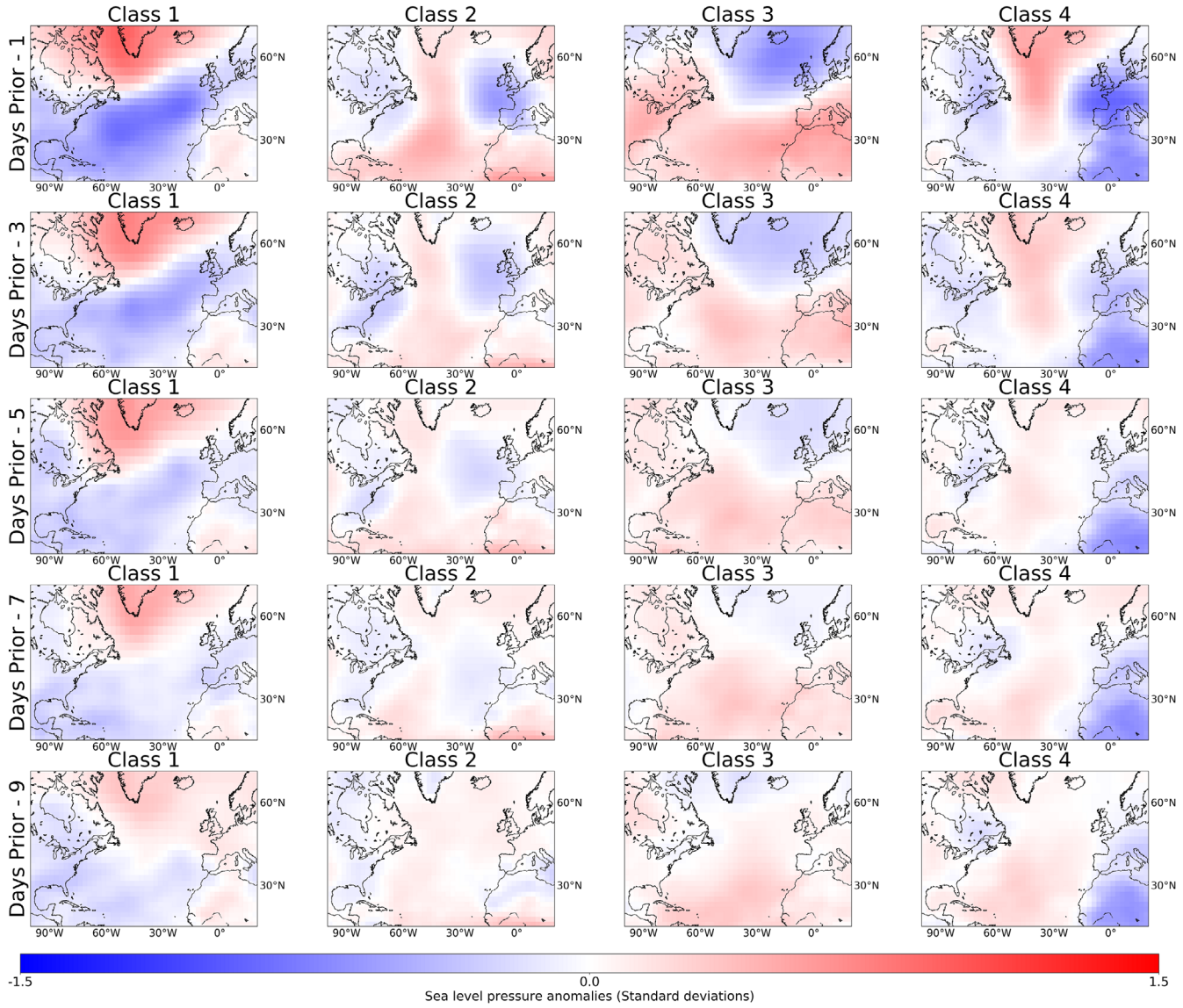

FIGURE 7 2 m air temperature anomalies in the North Atlantic region in the 1, 3, 5, 7 and 9 days prior to the heavy rainfall event occurring, for the four summer classes [Colour figure can be viewed at wileyonlinelibrary.com]

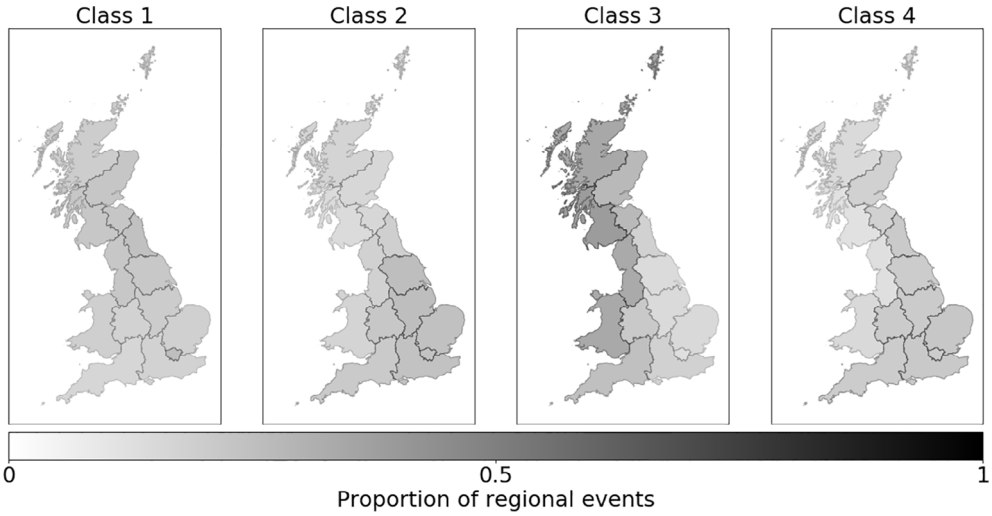

FIGURE 8 Geographical distribution of heavy rainfall events for each of the four summer classes, for each of 13 administrative regions of Great Britain (regions as in Hollis *et al.* (2019)). A high opacity indicates a higher proportion of event occurrence

in the south and east of Britain, which is consistent with cyclones tracking across southern Britain. Mesoscale convective systems, such as associated with the Spanish Plume (e.g., Lewis and Gray, 2010), mainly occur in southern Britain. However, although some classes have a warmer average temperature anomaly in western Europe and/or North Africa than others, the rarity of these events make it difficult to link them to any particular class.

The geographical distribution of heavy rainfall events associated with Class 3, whose spatial SLP pattern reflects the positive NAO, is concentrated to the north and west of the country (Figure 8). Here, heavy rain is likely produced along the fronts of cyclones travelling eastward, or northeastward, along a path to the north, between Scotland and Iceland, as suggested by the location of the low pressure anomaly in Figure 3 and the direction of the upper-level airflow in Figure 5.

Heavy rainfall for Class 1 events, which are closely associated with the negative NAO, are more evenly spread across Britain (Figure 8). For this class, the location of the low pressure anomaly in Figure 3 suggests a track slightly further to the south of those in Class 3.

Figure S5 shows box-and-whisker plots of the standardized summer rainfall maxima for the 13 regions, separately for each of the four classes. There is not much difference in the magnitude of the standardized rainfall maxima between the regions, but rather, as shown in Figure 8, the difference is in the frequency of occurrence. Because we have not extracted a seasonal maximum for each class, we are unable to do a formal frequency analysis.

4.2 | Winter

4.2.1 | Meteorological conditions

The anomaly and raw SLP patterns for the three winter classes are shown in Figure 9. Both the anomaly and raw SLP patterns show a low SLP value on, or northwest of, the British Isles. In the raw patterns (Figure 9b) Class 1 shows a considerably stronger low SLP between Scotland and Iceland than any of the other classes, a pattern which is replicated in summer Class 3. The corresponding pressure anomalies in Figure 9a show a similar pattern, with

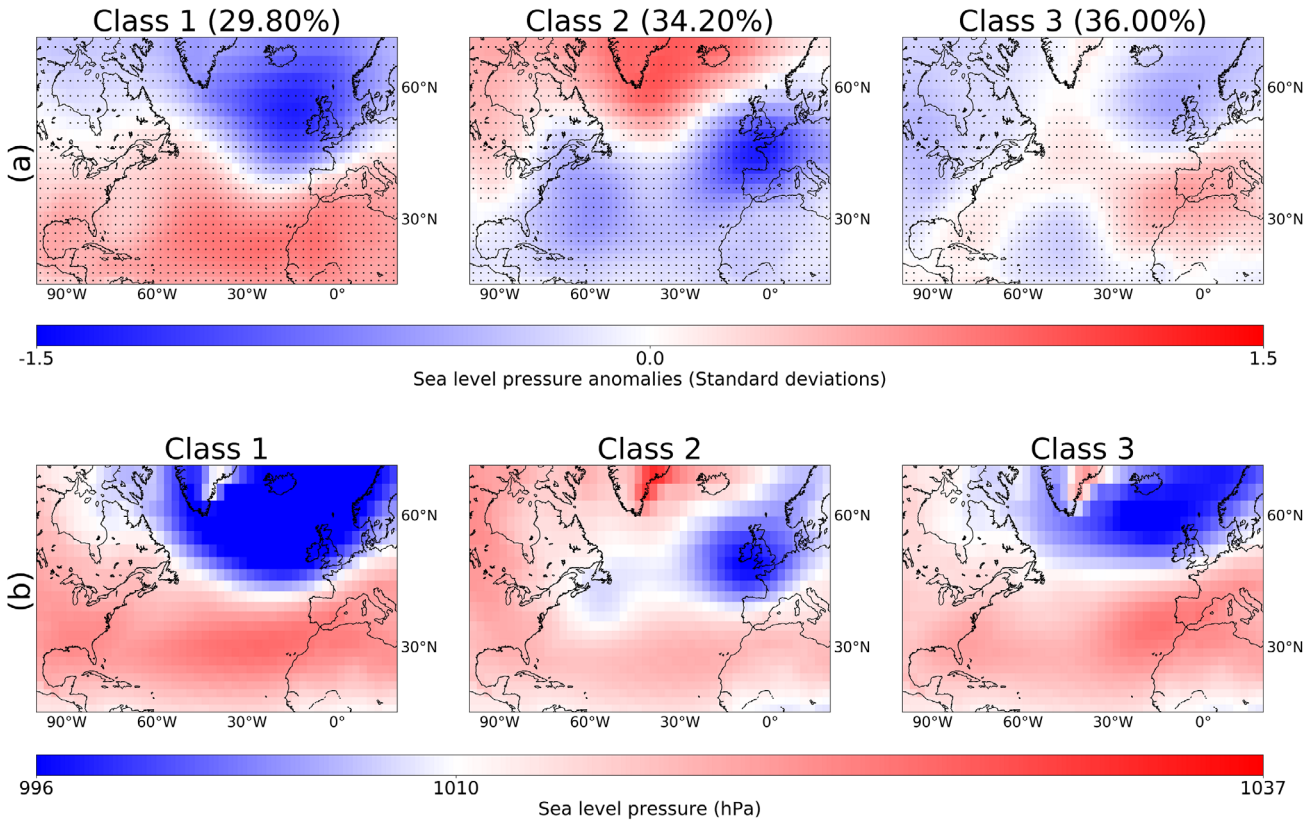

FIGURE 9 Sea-level pressure patterns for the three winter classes, showing both the anomaly SLP (a) and raw SLP (b) patterns. The percentages indicate the proportion of events in each class and the dots provided in (a) show the anomalies with a 2% significance value using a two-sided Student's *t* test [Colour figure can be viewed at wileyonlinelibrary.com]

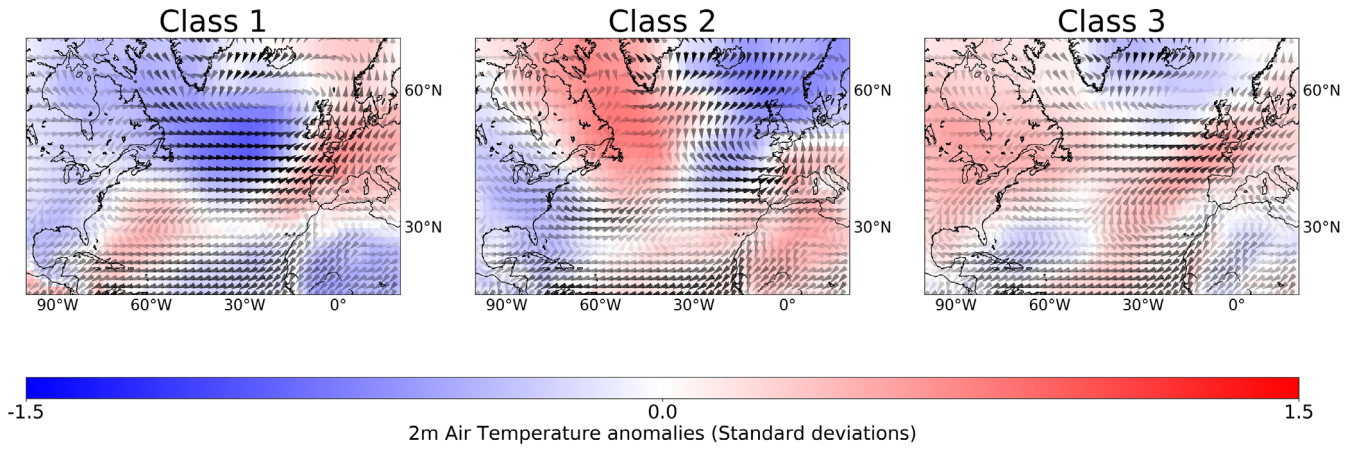

FIGURE 10 As Figure 6, but for the three winter classes. Anomaly 2 m air temperature patterns are shown without wind speeds, but with points denoting significance, in Supplementary Information S2 [Colour figure can be viewed at wileyonlinelibrary.com]

strong negative anomalies between Scotland and Iceland and positive anomalies over the Azores in the subtropical North Atlantic. In contrast, the pressure anomaly pattern for Class 2 shows positive anomalies over Iceland and negative anomalies to the south. The spatial patterns formed by the pressure anomalies in Classes 1 and 2 are consistent with the positive and negative phases of the NAO, respectively (e.g., Barnston and Livezey, 1987). Class 3 has similarities to the positive NAO pattern, but it is less pronounced than the Class 1 pattern, and the centre of the subtropical high pressure anomaly is shifted northeastwards, extending onto the Iberian peninsula and making it more reminiscent of the rotated summer NAO pattern.

For all three winter classes, the large-scale temperature patterns shown in Figure 10 are reminiscent of the Atlantic SST tripole pattern, with centres east of Newfoundland, near the southeastern coast of the United States, and in the tropical eastern Atlantic (e.g., Fan and Schneider, 2012). In addition, there is an area north of the UK (sometimes extending southwards) with a temperature anomaly of the same sign as the centre off the southeastern United States. The land areas near the Newfoundland and tropical east Atlantic tripole centres support the SST anomaly, but for the other two centres the temperature of the neighbouring land areas may differ. The wind pattern shown in Figure 10 confirms a northeastward shift of the subtropical high pressure for Class 3.

Locally near the UK, all three classes show warm temperature anomalies either across the UK and/or to the south, and southwesterly or southerly winds transporting warm air towards the UK (Figure 10). For all three classes there are cold temperature anomalies to the west and/or northwest of the UK. The resulting temperature contrast between these air masses provides ideal conditions for heavy rainfall at the cold front or low-pressure centre of a mid-latitude cyclone. Figure 9 suggests that for Class 2 the low pressure is located over Great Britain, whereas for Classes 1 and 3 it is centred further to the north and it may be the trailing cold front that is mainly responsible for the heavy rainfall event. A difference between Classes 1 and 3 is the strength and location of the cold anomaly, which is relatively weak and centred over Iceland for Class 3 but is very strong and located to the southwest of Iceland for Class 1. The temporal evolution of the temperature anomalies (Figure 11) suggests that for Class 3 the anomaly develops within the last few days before the heavy rainfall event occurs, but for Class 1 the cold anomaly has existed in the same location for at least the past 10 days. Supplementary Information S4 shows the corresponding development of sea level pressure anomalies in the days prior to the heavy rainfall event.

Figure 12 shows the 500 hPa geopotential heights for the three classes. For Class 2 the figure suggests a meandering storm track which is consistent with a negative NAO. In contrast, the storms for Classes 1 and 3 have travelled along a nearly straight path from a westerly to southwesterly direction.

4.2.2 | Class variability

The top row of Figure 13 shows how the frequency of occurrence of the events in each winter class varies with time, while the lower two rows show how the detrended frequencies of occurrence vary with the detrended indices of the NAO and AMO. The frequency of Class 1 increases significantly with time, whereas the frequency of Class 2 decreases significantly and Class 3 shows no temporal

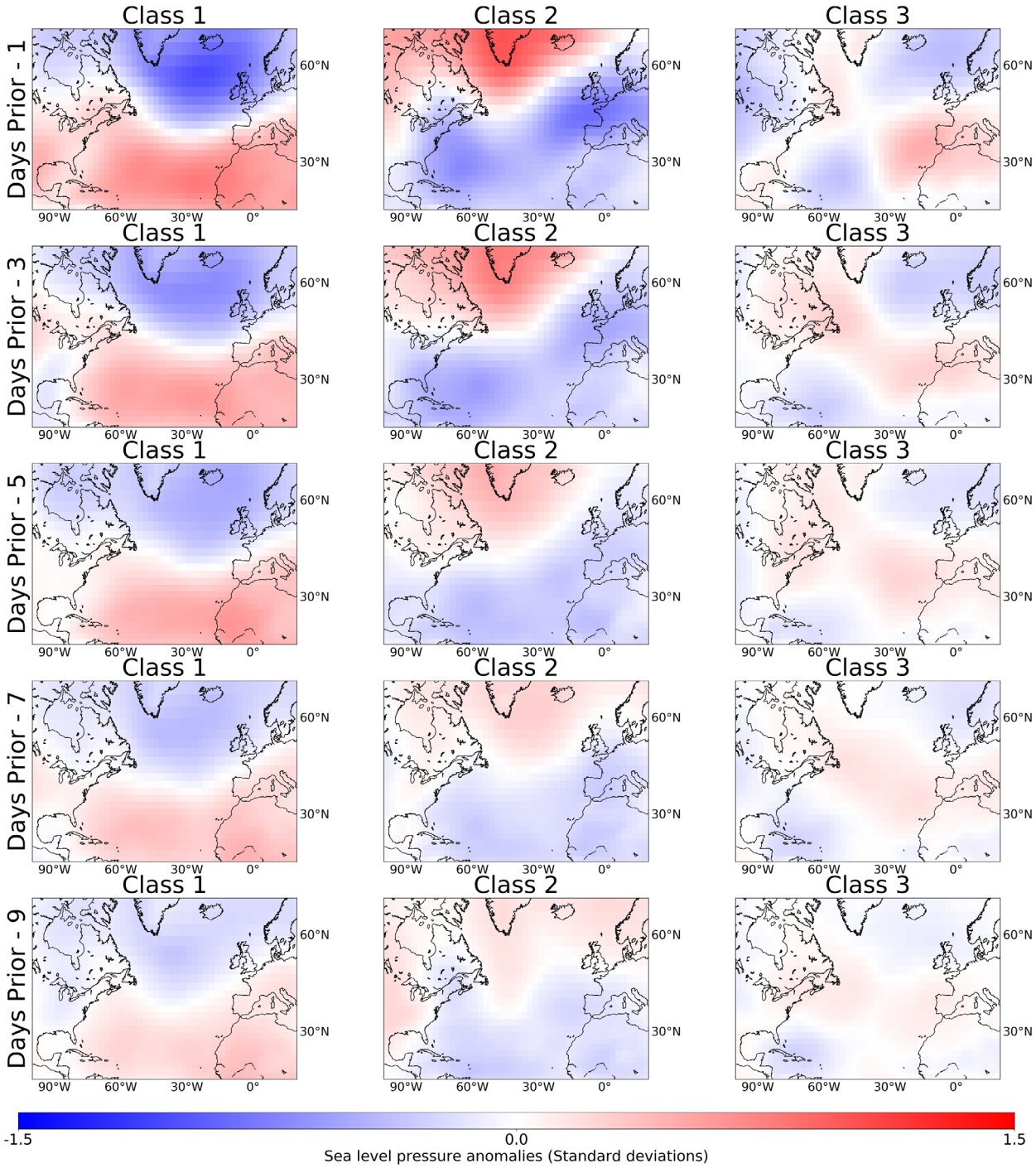

FIGURE 11 2 m air temperature anomalies in the North Atlantic region in the 1, 3, 5, 7 and 9 days prior to the heavy rainfall event occurring, for the three winter classes [Colour figure can be viewed at wileyonlinelibrary.com]

trend. The detrended event frequencies of Classes 1 and 2 show a moderately strong dependence (significant at the 5 and 10% levels, respectively) with the detrended NAO index, with Class 1 events occurring more frequently during the positive NAO phase and Class 2 events occurring more frequently during the negative phase. This is consistent with the spatial SLP anomaly patterns in Figure 9a. In contrast, for Class 3 there is no significant correlation with either time or the two climate indices.

Somewhat unexpectedly for winter, we find a significant negative association with the AMO for Class 1. The cold temperature anomaly in the northwest Atlantic for winter Class 1 has persisted for at least 10 days (Figure 11), and it is possible that it may be so long-lasting and widespread that it influences the estimate of

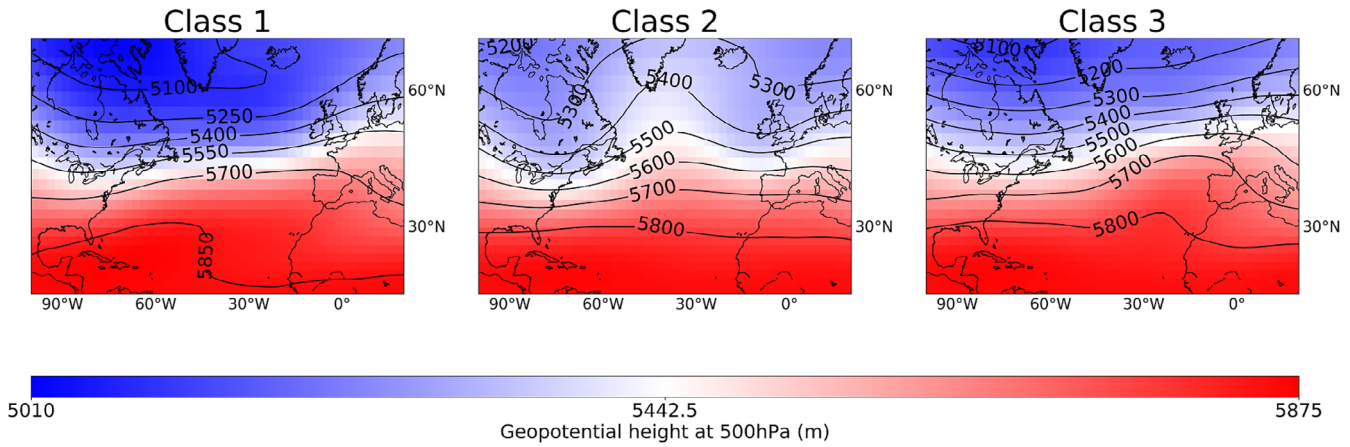

FIGURE 12 500 hPa geopotential heights for each winter class [Colour figure can be viewed at wileyonlinelibrary.com]

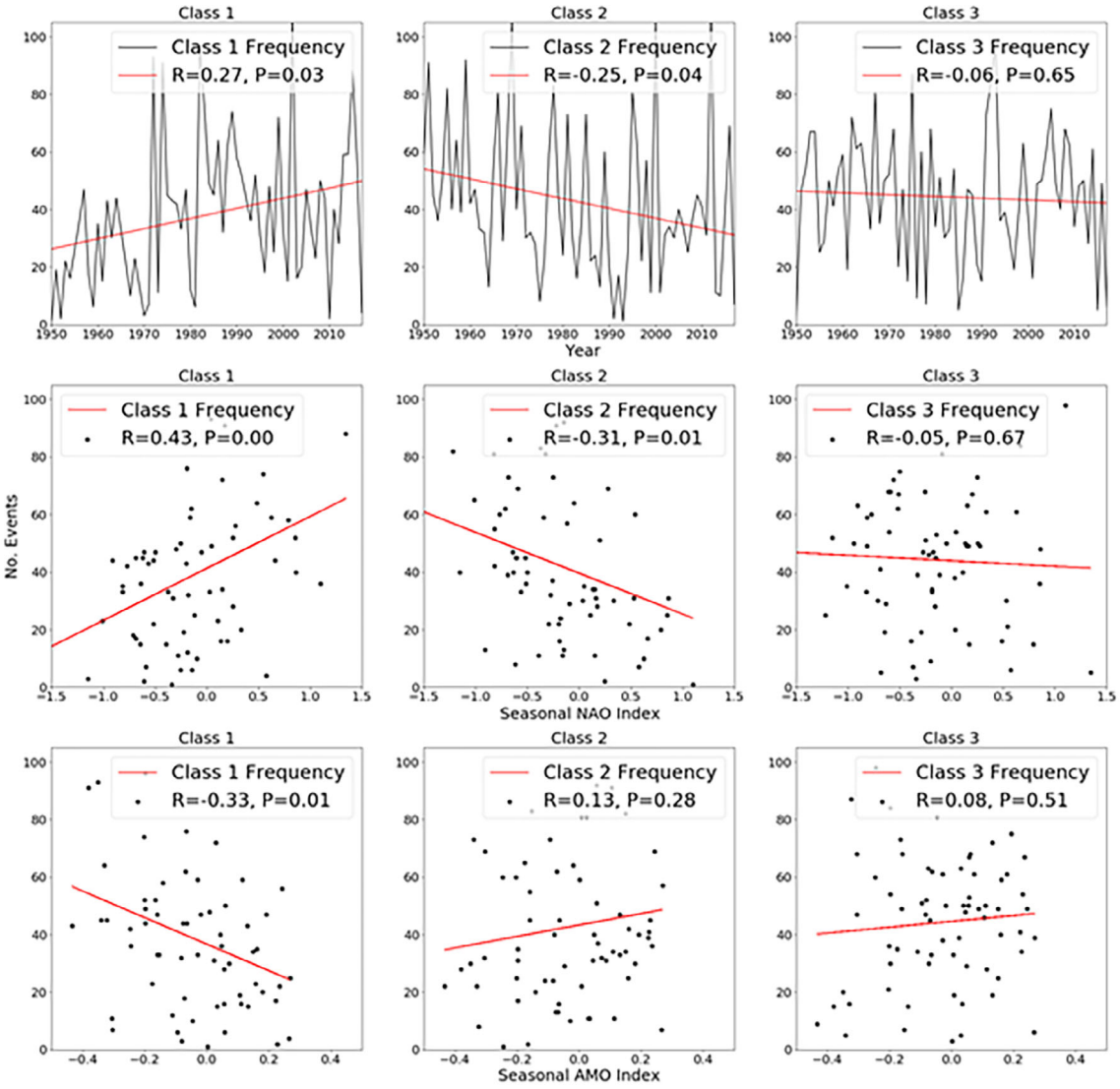

FIGURE 13 As Figure 6, but for the three winter classes [Colour figure can be viewed at wileyonlinelibrary.com]

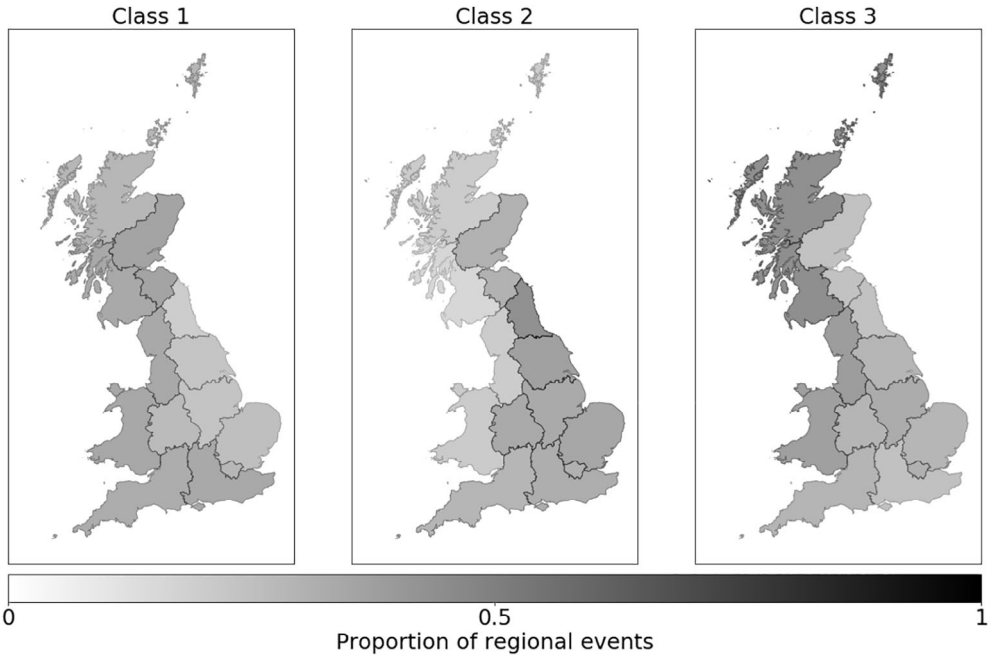

FIGURE 14 Geographical distribution of heavy rainfall events for each of the three winter classes for each of 13 administrative regions of Great Britain. A high opacity indicates a higher proportion of event occurrence

the AMO index for the season. The negative correlation with the AMO, and the positive correlation with the NAO, for Class 1 in winter is similar to the correlations for Class 3 in summer. The pressure patterns for these classes are also similar (Figures 3 and 9).

Comparing the frequency of occurrence regionally across Great Britain (Figure 14) reveals different distributions for each of the three classes. Heavy rainfall events in Class 2 show a preference for occurring in the south and east, as can be expected for a SLP pattern reflecting the negative phase of the NAO. The location of the SLP anomaly in Figure 9 suggests cyclones are tracking across Britain, and prolonged rainfall in eastern Britain often occurs in onshore winds on the northern side of depressions (e.g., Wheeler, 1997).

Class 1 events cause heavy rainfalls mainly in western Britain, with their low-pressure centres located further north compared with events in Class 2 (Figure 9). Class 3 events are concentrated in the far northwest, and the spatial rainfall distribution is rather similar to that for the summer Class 3 events. The SLP patterns for both summer Class 3 (Figure 3) and winter Class 3 (Figure 9) display a slight counter-clockwise rotation of the high pressure centre (shifted northeastwards from the North Atlantic onto the Iberian peninsula) compared with the more standard winter NAO pattern of Class 1. This seems to shift the low pressure, and the main rainfall area, slightly further north for Class 3 compared with Class 1.

Again, similarly to summer, there is not much difference in the magnitude of the standardized winter rainfall maxima for the 13 regions, for the three winter classes (Figure S6). The difference is in the regional frequency of occurrence (Figure 14).

5 | DISCUSSION

Including 2 m air temperature across the North Atlantic sector as an extra feature set to the meteorological clustering, which is traditionally done only on atmospheric pressure patterns, has provided a new view of the conditions leading to heavy rainfall events in Great Britain. The four identified classes in summer, and the three classes in winter, are each associated with different geographical distributions of heavy rainfall events. The temperature and circulation patterns identified in this study indicate local areas whose temperature and/or pressure has the potential to be used as additional predictors for weather generators such as for example described by Serinaldi and Kilsby (2012). Future work could also involve investigating the large-scale temperature and pressure patterns predicted by global climate models, and the expected effect these would have on heavy rainfall characteristics in different parts of Britain.

In this context we compare the circulation patterns derived in the present study using both the SLP and 2 m air temperature anomalies, with the classes from previous studies which are based on atmospheric circulation only, but for which the associated UK rainfall has also been assessed (Sections 5.1 and 5.2). We then discuss the sensitivity of the results to the choices of data and methods (Section 5.3).

5.1 | Summer

Neal *et al*. (2016) present 30 circulation patterns over the North Atlantic – European region, for which Richardson *et al*. (2017) calculate regional UK median rainfall and rainfall variability (inter-quartile range). Our summer Classes 1, 2, 3 and 4 show some similarities in SLP anomalies (Figure 4) and wind directions (Figure 5), with circulation patterns number N28, N29, N21 and N11, respectively, identified by Neal *et al*. (2016) (an 'N' has been inserted before the pattern number to distinguish them from our Classes). Richardson *et al*. (2017) show that patterns N29 and N21 are both associated with high rainfalls in most of the country, but for N29 particularly in the south and east, and for N21 particularly in the north and west. This is in general agreement with the rainfall distributions for our Classes 2 and 3, respectively (Figure 8). For patterns N28 and N11 Richardson *et al*. (2017) find that rain mainly falls in the south and east (similar to our Classes 1 and 4), but the median rainfall is only moderate. However, the rainfall variability is rather high, which suggests that the patterns include both wet and dry events. Since the Classes in our study are by design associated with high rainfall events, a contributing factor to distinguishing between the wet and dry events in Neal et al.'s patterns may be the temperature patterns associated with our Classes (Figure 5).

5.2 | Winter

Despite the significant correlation with the NAO, the winter Class 1 seems to have more similarities with Neal *et al*. (2016)'s pattern N21 than with the six patterns they label typical of the positive NAO phase; Class 1 has a southwesterly, rather than westerly, wind direction over the UK. The winter Class 2 has similarities to Neal *et al*. (2016)'s pattern N11, and Class 3 to pattern N2 (which is similar to N21, but has a weaker low pressure). The principal rainfall areas largely overlap for Class 1 and N21 (north and west) and Class 2 and N11 (south and east). The rainy regions for Class 3 and N2 are both mainly in the north and west of the country, and for pattern N2 Richardson *et al*. (2017) again suggest a combination of a moderate rainfall median and a higher rainfall variability.

For winter, further comparisons can be made between our classes and those found by Ummenhofer *et al*. (2017), who show circulation patterns and associated rainfall patterns over Europe. However, these comparisons are less clear due to the fewer and more generalized classes used by Ummenhofer et al., and the disparity in spatial rainfall domain. The circulation patterns (Figures 10 and 11) of our Classes 1 and 3 both show similarities to UB and UE, and Class 2 to UC, where U*i* indicates pattern *i* in Ummenhofer *et al*. (2017). The strongest similarities are between Class 2 and UC, which is also reflected in the regional distribution of rainfall which favours eastern and southern Britain (Figure 14). Classes 1 and 3, and UB and UE, all occur mainly in the north and west of Britain.

5.3 | Sensitivity of the results to data and methods choices

The results of the study are sensitive to the selection of data and methods. Non-stationarity of the data means that the period of record used will influence the classification results, including the derived quantities such as rainfall magnitude and geographical distribution associated with each class. Figures 6 and 13 show how the number of events in each class vary with time. We have explored two potential co-variates that are known to influence the region, the NAO and AMO climate indices, but other oscillations and phenomena have not been investigated.

Some subjective choices have been made regarding the clustering algorithm, initialization conditions and the preselection of atmospheric variables. The algorithm used (*k*-means) will tend to generate clusters of roughly equal size, and the results depend heavily on the initial number of clusters chosen, *k*. In this study, we chose a *k*-value based on subjective analysis of the clustering results, and the results of earlier studies as discussed in Section 3.2.

Other factors which influence the sensitivity of the analysis include the spatial domain and the product from which the meteorological data was extracted. As we wanted to investigate also the influence of temperature on land areas neighbouring the North Atlantic, we selected a larger domain than used in some earlier studies (e.g., Richardson *et al*., 2017; Ummenhofer *et al*., 2017), and this will have affected the results compared with those studies. We used the NCEP/NCAR Reanalysis 1 product for the meteorological data, but different results may have been found if, for example, a similar reanalysis product from the European Centre for Medium range Weather Forecasts (ECMWF) had been used, or if moisture rather than temperature data had been used.

6 | SUMMARY AND CONCLUSIONS

Meteorological conditions over the North Atlantic were extracted from NCEP/NCAR Reanalysis Data (Kalnay *et al*., 1996) for seasonal heavy rainfall events (summer and winter 1-day maxima) at 125 locations across Great Britain. The anomaly sea level pressure and 2 m air

temperature patterns associated with each event were clustered jointly to find how the meteorological conditions over the North Atlantic sector co-vary to produce heavy rainfall events.

Four classes were identified for summer. Two of them suggest that heavy rainfalls are affected by opposing combinations of the seasonal NAO and AMO: negative (positive) NAO and positive (negative) AMO for Class 1 (Class 3). The remaining Classes 2 and 4 are both associated with a northward extension of the subtropical high pressure in the North Atlantic, highly meandering storm tracks, and heavy rainfall predominantly in southeast Britain. Although these classes are associated with opposing North Atlantic temperatures (Figure 4), only the event frequency for Class 2 is significantly correlated (at the 10% level) with the seasonal AMO.

Whereas in summer the temperature patterns show either predominantly cold or warm anomalies over most of the North Atlantic, in winter two phases of a smaller-scale four-pole temperature pattern emerges. This resembles the SST tripole pattern (e.g., Fan and Schneider, 2012), plus a centre north of the UK with a temperature anomaly of the same sign as the centre off the southeastern United States.

The number of events in winter Class 1 shows significant positive correlation with the NAO and negative correlation with the AMO. There is a strong, widespread and persistent cold anomaly in the SST centre off Newfoundland, which may influence the seasonal AMO index. Heavy rainfall events mainly occur in western Britain. In contrast, the number of Class 2 events is significantly (10% level) negatively correlated with the NAO, and the meandering storm tracks result in heavy rainfall mainly in the south and east.

The pressure pattern for winter Class 3 shows some similarity with that typical of the positive phase of the NAO, but with the subtropical high-pressure anomaly shifted eastwards onto western Europe. There is no correlation with either the NAO or AMO. The pressure pattern is similar to the summer Class 3 pattern, and both these classes result in a strong focus of heavy rainfall events in the northwest of Great Britain. The cold temperature anomaly to the northwest of the UK develops over a matter of days prior to the heavy rainfall occurring, similar to the events in summer, and in contrast to the longer-lasting cold anomaly of winter Class 1.

ACKNOWLEDGEMENTS

The authors gratefully acknowledge the NCEP Reanalysis, NAO and AMO data provided by the NOAA/OAR/ESRL PSD, Boulder, Colorado, USA, from their website at https://www.esrl.noaa.gov/psd/ as well as the CEH-GEAR rainfall dataset provided by UKCEH, available through their website at https://catalogue.ceh.ac.uk/documents/ee9ab43d-a4fe-4e73-afd5-cd4fc4c82556. Andrew Barnes acknowledges funding as part of the Water Informatics Science and Engineering Centre for Doctoral Training (WISE CDT) under a grant from the Engineering and Physical Sciences Research Council (EPSRC), grant number EP/L016214/1. The contributions by Cecilia Svensson were supported by the UK Natural Environment Research Council (NERC) National Capability award NE/R016429/1, UK-SCAPE (UK Status, Change and Projections of the Environment), https://www.ceh.ac.uk/ukscape.

AUTHOR CONTRIBUTIONS

Andrew Paul Barnes: Conceptualization; data curation; formal analysis; funding acquisition; investigation; methodology; project administration; resources; software; validation; visualization; writing – original draft; writing – review and editing. **Cecilia Svensson:** Conceptualization; formal analysis; investigation; project administration; supervision; writing – original draft; writing – review and editing. **Thomas Rodding Kjeldsen:** Conceptualization; project administration; supervision; writing – original draft; writing – review and editing.

ORCID

Andrew Paul Barnes https://orcid.org/0000-0002-1709-5304
Cecilia Svensson https://orcid.org/0000-0001-9294-5826
Thomas Rodding Kjeldsen https://orcid.org/0000-0001-9423-5203

REFERENCES

Aggarwal, C. C., Hinneburg, A., & Keim, D. A. (2001) On the surprising behavior of distance metrics in high dimensional space. *International Conference on Database Theory*. pp. 420–434. https://doi.org/10.1007/3-540-44503-X_27

Allan, R.P., Blenkinsop, S., Fowler, H.J. and Champion, A.J. (2019) Atmospheric precursors for intense summer rainfall over the United Kingdom. *International Journal of Climatology*, 40, 1–19. https://doi.org/10.1002/joc.6431.

Barnes, A. P., McCullen, N., & Kjeldsen, T. R. (2019a) The atmospheric origins of extreme rainfall in the UK. *Proceedings of the IMA's 4th International Flood Risk Conference*.

Barnes, A.P., Santos, M.S., Garijo, C., Mediero, L., Prosdocimi, I., McCullen, N. and Kjeldsen, T.R. (2019b) Identifying the origins of extreme rainfall using storm track classification. *Journal of Hydroinformatics*, 22, 296–309. https://doi.org/10.2166/hydro.2019.164.

Barnston, A.G. and Livezey, R.E. (1987) Classification, seasonality and persistence of low-frequency atmospheric circulation patterns. *Monthly Weather Review*, 115(6), 1083–1126.

Blenkinsop, S., Chan, S.C., Kendon, E.J., Roberts, N.M. and Fowler, H.J. (2015) Temperature influences on intense UK hourly precipitation and dependency on large-scale circulation. *Environmental Research Letters*, 10(5), 054021. https://doi.org/10.1088/1748-9326/10/5/054021.

Champion, A.J., Blenkinsop, S., Li, X.-F. and Fowler, H.J. (2019) Synoptic-scale precursors of extreme U.K. summer 3-hourly rainfall. *Journal of Geophysical Research: Atmospheres*, 124, 4477–4489. https://doi.org/10.1029/2018JD029664.

Enfield, D.B., Mestas-Nuñez, A.M. and Trimble, P.J. (2001) The Atlantic multidecadal oscillation and its relation to rainfall and river flows in the continental U.S. *Geophysical Research Letters*, 28(10), 2077–2080. https://doi.org/10.1029/2000GL012745.

Fan, M. and Schneider, E.K. (2012) Observed decadal North Atlantic tripole SST variability. Part I: weather noise forcing and coupled response. *Journal of the Atmospheric Sciences*, 69, 35–50. https://doi.org/10.1175/JAS-D-11-018.1.

Fereday, D.R., Knight, J.R., Scaife, A.A., Folland, C.K. and Philipp, A. (2008) Cluster analysis of North Atlantic European circulation types and links with tropical Pacific Sea surface temperatures. *Journal of Climate*, 21(15), 3687–3703. https://doi.org/10.1175/2007JCLI1875.1.

Folland, C.K., Knight, J., Linderholm, H.W., Fereday, D., Ineson, S. and Hurrell, J.W. (2009) The summer North Atlantic oscillation: past, present, and future. *Journal of Climate*, 22, 1082–1103. https://doi.org/10.1175/2008JCLI2459.1.

Gimeno, L., Vázquez, M., Eiras-Barca, J., Sorí, R., Stojanovic, M., Algarra, I., Nieto, R., Ramos, A.M., Durán-Quesada, A.M. and Dominguez, F. (2020) Recent progress on the sources of continental precipitation as revealed by moisture transport analysis. *Earth-Science Reviews*, 201, 103070. https://doi.org/10.1016/j.earscirev.2019.103070.

Greco, A., De Luca, D.L. and Avolio, E. (2020) Heavy precipitation systems in Calabria Region (southern Italy): high-resolution observed rainfall and large-scale atmospheric pattern analysis. *Water*, 12(5), 1468. https://doi.org/10.3390/w12051468.

Griffith, H. (2020) *A month of storms: Ciara, Dennis and atmospheric rivers*. Available at: https://hepex.inrae.fr/atm-rivers-ciara-dennis/ [Accessed 28th August 2020].

Hollis, D., McCarthy, M., Kendon, M., Legg, T. and Simpson, I. (2019) HadUK-grid—A new UK dataset of gridded climate observations. *Geoscience Data Journal*, 6(2), 151–159. https://doi.org/10.1002/gdj3.78.

Jenkinson, A.F. and Collison, F.P. (1977) An initial climatology of gales over the North Sea. In: *Synoptic Climatology Branch Memorandum No. 62*. Bracknell: Meteorological Office.

Jones, P.D., Jonsson, T. and Wheeler, D. (1997) Extension to the North Atlantic oscillation using early instrumental pressure observations from Gibraltar and south-west Iceland. *International Journal of Climatology*, 17(13), 1433–1450. https://doi.org/10.1002/(SICI)1097-0088(19971115)17:13<1433::AID-JOC203>3.0.CO;2-P.

Kalnay, E., Kanamitsu, M., Kistler, R., Collins, W., Deaven, D., Gandin, L., Iredell, M., Saha, S., White, G., Woollen, J., Zhu, Y., Chelliah, M., Ebisuzaki, W., Higgins, W., Janowiak, J., Mo, K. C., Ropelewski, C., Wang, J., Leetmaa, A., Jenny, R. and Joseph, D. (1996) The NCEP/NCAR 40-year reanalysis project. *Bulletin of the American Meteorological Society*, 77(3), 437–472. https://doi.org/10.1175/1520-0477(1996)077.

Kaplan, A., Cane, M., Kushnir, Y., Clement, A., Blumenthal, M. and Rajagopalan, B. (1998) Analyses of global sea surface temperature 1856–1991. *Journal of Geophysical Research, Oceans*, 103(C9), 18,567–18,589.

Keef, C., Svensson, C. and Tawn, J.A. (2009) Spatial dependence in extreme river flows and precipitation for Great Britain. *Journal of Hydrology*, 378(3–4), 240–252. https://doi.org/10.1016/j.jhydrol.2009.09.026.

Keller, V.D.J., Tanguy, M., Prosdocimi, I., Terry, J.A., Hitt, O., Cole, S.J., Fry, M., Morris, D.G. and Dixon, H. (2015) CEH-GEAR: 1 km resolution daily and monthly areal rainfall estimates for the UK for hydrological and other applications. *Earth System Science Data*, 7, 143–155. https://doi.org/10.5194/essd-7-143-2015.

Lamb, H.H. (1965) The English climate. By H. H. Lamb. London (English Universities Press). Second (rewritten) edition, 1964. Pp. ix, 212; 30 Figures; 3 Appendices. 12s. 6d paperback; 21s. cloth bound. *Quarterly Journal of the Royal Meteorological Society*, 91(388), 252. https://doi.org/10.1002/qj.49709138829.

Lamb, H. H. (1972) *British Isles Weather Types and a Register of the Daily Sequence of Circulation Patterns 1861–1971*. H.M. Stationary Office: Geophysical Memoires.

Lavers, D.A., Allan, R.P., Wood, E.F., Villarini, G., Brayshaw, D.J. and Wade, A.J. (2011) Winter floods in Britain are connected to atmospheric rivers. *Geophysical Research Letters*, 38(23). https://doi.org/10.1029/2011GL049783.

Lavers, D.A. and Villarini, G. (2015) The contribution of atmospheric rivers to precipitation in Europe and the United States. *Journal of Hydrology*, 522, 382–390. https://doi.org/10.1016/j.jhydrol.2014.12.010.

Lewis, M.W. and Gray, S.L. (2010) Categorisation of synoptic environments associated with mesoscale convective systems over the UK. *Atmospheric Research*, 97(1–2), 194–213. https://doi.org/10.1016/j.atmosres.2010.04.001.

Lloyd, S. (1982) Least squares quantization in PCM. *IEEE Transactions on Information Theory*, 28(2), 129–137. https://doi.org/10.1109/TIT.1982.1056489.

Long-term investment scenarios (LTIS). (2019) Environment Agency, https://www.gov.uk/government/publications/flood-and-coastal-risk-management-in-england-long-term-investment/long-term-investment-scenarios-ltis-2019. Updated 8 May 2019 [Accessed 27th January 2020].

Neal, R., Fereday, D., Crocker, R. and Comer, R.E. (2016) A flexible approach to defining weather patterns and their application in weather forecasting over Europe. *Meteorological Applications*, 23(3), 389–400. https://doi.org/10.1002/met.1563.

NOAA National Weather Service. (2005) *North Atlantic Oscillation (NAO)*. Available at: https://www.cpc.ncep.noaa.gov/products/precip/CWlink/pna/nao.shtml.

Richardson, D., Fowler, H.J., Kilsby, C.G. and Neal, R. (2017) A new precipitation and drought climatology based on weather patterns. *International Journal of Climatology*, 38(2), 630–648.

Santos, M., Mediero, L., Lima, C. and Zandonadi Moura, L. (2018) Links between different classes of storm tracks and the flood trends in Spain. *Journal of Hydrology*, 567, 71–85. https://doi.org/10.1016/j.jhydrol.2018.10.003.

Serinaldi, F. and Kilsby, C.G. (2012) A modular class of multisite monthly rainfall generators for water resource management and impact studies. *Journal of Hydrology*, 464–465, 528–540. https://doi.org/10.1016/j.jhydrol.2012.07.043.

Svensson, C. and Hannaford, J. (2019) Oceanic conditions associated with Euro-Atlantic high pressure and {UK} drought. *Environmental Research Communications*, 1(10), 101001. https://doi.org/10.1088/2515-7620/ab42f7.

Tan, X., Gan, T.Y. and Chen, Y.D. (2018) Moisture sources and pathways associated with the spatial variability of seasonal extreme precipitation over Canada. *Climate Dynamics*, 50(1–2), 629–640. https://doi.org/10.1007/s00382-017-3630-0.

Tanguy, M., Dixon, H., Prosdocimi, I., Morri, D. G., and Kelle, V. D. J. (2019) Gridded estimates of daily and monthly areal rainfall for the United Kingdom (1890-2017) [CEH-GEAR]. NERC Environmental Information Data Centre. https://doi.org/10.5285/ee9ab43d-a4fe-4e73-afd5-cd4fc4c82556

Taylor, J.A. and Yates, R.A. (1967) *British Weather in Maps*. New York: Macmillan.

Tramblay, Y., Neppel, L., Carreau, J. and Najib, K. (2013) Non-stationary frequency analysis of heavy rainfall events in southern France. *Hydrological Sciences Journal*, 58(2), 280–294. https://doi.org/10.1080/02626667.2012.754988.

Ummenhofer, C.C., Seo, H., Kwon, Y.-O., Parfitt, R., Brands, S. and Joyce, T.M. (2017) Emerging European winter precipitation pattern linked to atmospheric circulation changes over the North Atlantic region in recent decades. *Geophysical Research Letters*, 44, 8557–8566. https://doi.org/10.1002/2017GL074188.

Wheeler, D. (1997) North-east England and Yorkshire. In: Wheeler, D. and Mayes, J. (Eds.) *Regional Climates of the British Isles*. London: Routledge, pp. 158–180.

SUPPORTING INFORMATION

Additional supporting information may be found in the online version of the article at the publisher's website.

How to cite this article: Barnes, A. P., Svensson, C., & Kjeldsen, T. R. (2022). North Atlantic air pressure and temperature conditions associated with heavy rainfall in Great Britain. *International Journal of Climatology*, *42*(5), 3190–3207. https://doi.org/10.1002/joc.7414